EurJIC European Journal of Inorganic Chemistry
ChemPubSoc Europe
FULL PAPER

DOI:10.1002/ejic.201403145

Tracing the Iron Nitrosyl Complex [Fe(2,2′-bipyridine)-(CN)$_3$(NO)]$^-$

Ana Foi,[a] Florencia Di Salvo,[a] Fabio Doctorovich,*[a] Tapashi G. Roy,[b] Kathrin Stirnat,[c] Christian Biewer,[c] and Axel Klein*[c]

Keywords: Iron / Nitrogen oxides / Diimines / Electrochemistry / IR spectroscopy

The previously reported complex [Ph$_4$P][Fe(bpy)(CN)$_3$(NO)] (bpy = 2,2′-bipyridine) was synthesised and characterised in detail using UV/Vis absorption and IR spectroscopy, cyclic voltammetry, and single-crystal XRD. Detailed spectroelectrochemical (UV/Vis, IR and EPR) insight adds perfectly to the previous electrochemical characterisation of this complex. The description of this {Fe(NO)}^{7} complex as a low-spin Fe^{II}–NO$^·$ system based on the spectroscopic results is supported by DFT calculations. Reversible oxidation leads to the corresponding {Fe(NO)}^{6} (Fe^{II}–NO$^+$) complex, whereas the reduction to the formal {Fe(NO)}^{8} species [presumably (Fe^{II}–NO$^-$)] occurs irreversibly. When trying to synthesise further derivatives that contain other α-diimine ligands, only for the 1,10-phenanthroline (phen) derivative were some results obtained. For other ligands the obtained materials were too reactive. The reasons for such behaviour are also discussed.

Introduction

Research on iron nitrosyl complexes is generally motivated by the interplay of iron and nitrosyl in biology, which, in chemical terms, could be described as the "taming" of the highly reactive nitrosyl molecule.[1–4] A very prominent scaffold for this purpose is provided by oligocyano iron species [Fe(CN)$_n$]$^{m-}$ ($5 > n > 3$; m depends both on n and the iron oxidation state) as in Na$_2$[Fe(CN)$_5$(NO)], the famous pentacyanonitrosyl ferrate(II), also called nitroprusside (NP), which has gained medicinal application as a highly effective hypotensive agent with few undesirable side effects.[1,5] The biological effect of NP is due to the release of NO in a physiologically controlled manner when administered. From the viewpoint of "taming" the nitrosyl, the nitrosyl-pentacyanoferrate platform [Fe(CN)$_5$(NO)]$^{m-}$ provides not only the possibility to generate coordinated nitrosyl in the NO$^+$, NO$^·$ or NO$^-$/HNO form,[6] it also allows one to carry out nitrosylation reactions.[7] At the same time, oligocyano iron complexes exhibit very specific properties, such as a very high sensitivity to the solvent surroundings[8] and they have been frequently used as building blocks in coordination chemistry.[9]

Starting from the nitrosyl-pentacyanoferrate, further platforms of the general type {MX$_5$(NO)} have been investigated to control the oxidation state of the nitrosyl ligand. Examples are {M(CN)$_5$(NO)} with M = Fe, Ru or Os[3,6,7,10–12] and {M′Cl$_5$(NO)} with M′ = Ir or Ru.[3c,13]

A further variation of the nitrosyl-pentacyanoferrate platform was previously presented by Fiedler and Mašek[10,11] with the complexes [Fe(N^N)(CN)$_3$(NO)]$^-$ [N^N = 2,2′-bipyridine (bpy) and 1,10-phenanthroline (phen)] in which two cyano ligands are replaced by the diimine chelate ligands to stabilise the {Fe(NO)}^{7} state (nomenclature by Enemark and Feltham[14]). The {Fe(NO)}^{7} species [Fe(CN)$_5$(NO)]$^{3-}$[3e,10,15,16] is highly reactive and rapidly cleaves cyanide. The idea was that the introduction of the π-backbonding diimine ligands might stabilise this oxidation state. They obtained the complexes from Na$_2$[Fe(CN)$_5$(NO)]·2H$_2$O ({Fe(NO)}^{6}), dithionite as a reductant and the corresponding diimine in aqueous solutions.[10,11] The products were precipitated by adding [Ph$_4$P]Br (Ph = phenyl) and isolated (yield was not provided). The electrochemistry of these compounds has been studied using polarography and some spectroscopic information and magnetic measurements gave insight into these interesting {Fe(NO)}^{7} complexes, which very likely contain low-spin Fe^{II} and NO$^·$. The bpy complex was oxidised using bromine to the very reactive and poorly characterised {Fe(NO)}^{6} complex [Fe(bpy)(CN)$_3$(NO)].[11]

[a] Departamento de Química Inorgánica, Analítica, y Química Física, Facultad de Ciencias Exactas y Naturales, Universidad de Buenos Aires, INQUIMAE-CONICET,
Ciudad Universitaria, Pabellón 2, Piso 3, C1428EHA Buenos Aires, Argentina
E-mail: doctorovich@qi.fcen.uba.ar
[b] University of Chittagong,
Chittagong 4331, Bangladesh
[c] Universität zu Köln, Institut für Anorganische Chemie,
Greinstraße 6, 50939 Köln
E-mail: axel.klein@uni-koeln.de
http://www.klein.uni-koeln.de/
Supporting information for this article is available on the WWW under http://dx.doi.org/10.1002/ejic.201403145.

© 0000 Wiley-VCH Verlag GmbH & Co. KGaA, Weinheim

In this work we present a complete characterisation of $[Ph_4P][Fe(bpy)(CN)_3(NO)]$ by single-crystal XRD structural studies, spectroelectrochemistry, and other spectroscopic techniques such as UV/Vis absorption, IR, and EPR.

In contrast to the complexes of the type $\{MX_5(NO)\}$, such a variable platform as $[Fe(N^N)(CN)_3(NO)]^{m-}$ might allow electronic variations of the nitrosyl ligand through alteration of the α-diimine ligand N^N. Therefore, we also sought to prepare similar analogues by varying the diimine ligands; however, it turned out that only the bpy and phen complexes were stable.

The results are discussed in comparison to $[Fe(CN)_5(NO)]^{3-}$[3e,15,16] and further $\{FeNO\}^7$ species[17–26] of which the non-heme, six-coordinate complexes $[Fe(pyN_4)(NO)]^{2+}$ {PyN_4 = 2,6-$C_5H_3N[CMe(CH_2NH_2)_2]_2$},[17] $[Fe(pyS_4)(NO)]$ {pyS_4 = 2,6-bis(2-mercaptophenylthiomethyl)pyridine-(2–)},[18] $[Fe(PaPy_3)(NO)](ClO_4)$ {$PaPy_3H$ = *N*,*N*-bis-(2-pyridylmethyl)amine-*N*-ethyl-2-pyridine-2-carboxamide},[19] $[Fe(TIM)(MeCN)(NO)]^{2+}$ (TIM = 2,3,9,10-tetramethyl-1,4,8,11-tetraazacyclodeca-1,3,8,10-tetraene),[20] $[Fe(N_3PyS)(NO)]^+$ {N_3PySH = *N*-[2-phenylthiolmethyl-*N*-(2-pyridinylmethyl-*N*,*N*-bis(2-pyridinylmethyl)methylamine)]},[21] $[Fe(N_4Py)(NO)]^{2+}$ {N_4Py = 1,1-di(2-pyridinyl)-*N*,*N*-bis(2-pyridinylmethyl)methanamine}[21] and the cyclam complexes $[Fe(cyclam\text{-}ac)(NO)](PF_6)$ (cyclam-acH = 1,4,8,11-tetraazacyclotetradecane-1-acetic acid) and *trans*-$[Fe(cyclam)(Cl)(NO)](ClO_4)$ (cyclam = 1,4,8,11-tetraazacyclotetradecane)[22] are worth mentioning.

Results and Discussion

Complex Synthesis and Structural Characterisation

$[Ph_4P][Fe(bpy)(CN)_3(NO)]$ (**1**) was obtained in reasonable yield as described in the Experimental Section. As a first approach to the structural and electronic characterisation, FTIR spectroscopy was used to monitor the reaction. The spectrum of the obtained compound showed a very distinct intense signal associated with a coordinated NO ligand at 1642 cm^{-1} (KBr pellet), and owing to the redshifting in comparison to the coordinated nitrosonium of the nitroprusside used as starting material, it was assigned to a reduced NO species.[3,22,27] The signals that correspond to the three cyano ligands were associated with a *fac* arrangement.

Crystals of **1** suitable for single-crystal X-ray diffraction experiments were obtained from ethanol/diethyl ether mixtures. The structure was solved in the orthorhombic space group $P2_12_12_1$ (no. 19) with results depicted in Figures 1 and 2 (data in Table S1 of the Supporting Information). The presence of only one counterion (a PPh_4^+ cation) establishes the charge of the iron complex as –1. The molecular structure shows a bent FeNO geometry with an ∠FeNO of 147.9(2)° and a relatively long *d*NO of 1.168(3) Å (Figure 1 and Table S2) in agreement with the hypothesis of the redox state assignment of the nitrosyl as NO^-.[3,15,17–19,21,23c,24,28] For similar reported complexes[15–21] the Fe–N–O angle is in the range 141–149°, whereas *d*NO goes from 1.006 up to 1.211 Å. Thus, the parameters found for the complex reported herein are in agreement with these reference values. The supramolecular packing is ruled by the non-conventional hydrogen bonds C–H(bpy)···ON [distance H(bpy)···O 2.558(2) Å, C–H–O angle 142.9(2)°] and C–H(bpy)···NC [distances H(bpy)···N 2.558(2) and 2.588(2) Å, ∠CHN 169.8(2) and 172.6(2)°, respectively], which gives rise to a 1D infinite chain along the crystallographic *a* axis (Figure 2). The interaction between chains is given by C–H-(bpy)···NC contacts [distances H(bpy)···N 2.640(2) and 2.639(3) Å, ∠CHN 124.9(2) and 121.1(2)°, respectively]. Then, owing to the displacement between these linear arrangements, the resultant motif is a 3D zigzag sheet (Figure S1). By taking into account the cations, the supramolecular structure reveals that they are intercalated in the aforementioned 3D array described by the anions. Each phosphonium cation interacts with two different iron complexes through C–H(bpy)···NC contacts; at the same time, each of one of these two anions are part of different 3D sheets. A clear view is obtained along axis *b* (Figure S2).

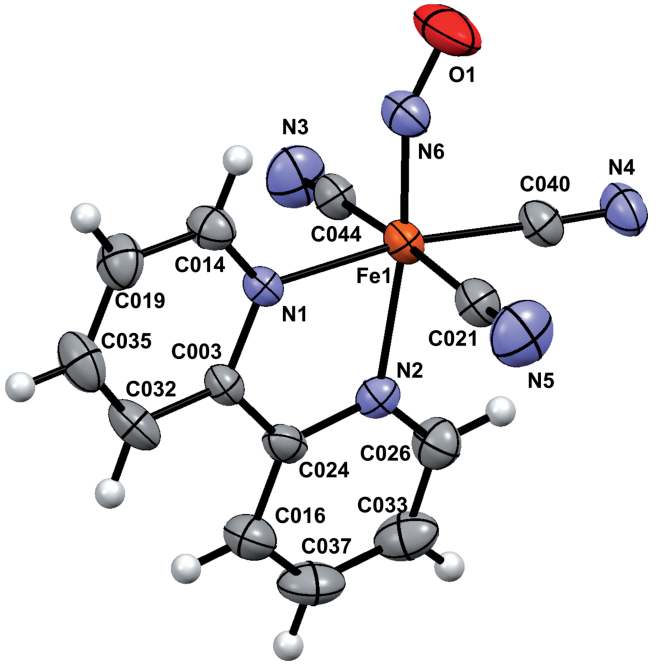

Figure 1. Molecular structure of $[Fe(bpy)(CN)_3(NO)]^-$ in $[Ph_4P][Fe(bpy)(CN)_3(NO)]$. All atoms at 50% probability level; protons were omitted for clarity. Selected bond lengths [Å] and angles [°]: Fe1–N1 2.037(2), Fe1–N2 2.125(2), Fe1–C021 1.961(3), Fe1–C040 1.925(3), Fe1–C044 1.959(3), N6–O1 1.168(3), C021–N5 1.143(3), C040–N4 1.137(3), C044–N3 1.151(3); Fe1–N6–O1 147.9(2), Fe1–C021–N5 175.8(2), Fe1–C040–N4 176.8(2), Fe1–C044–N3 176.7(2).

The synthesis of further compounds of the type $[Ph_4P][Fe(N^N)(CN)_3(NO)]$ with various α-diimine ligands N^N such as 1,10-phenanthroline (phen), dipyrido-[3,2-*a*:2′,3′-*c*]phenazine (dppz), *N*,*N*-disiopropyl-1,4-diazabutadiene (*i*Pr-DAB) or bis(mesityl)acenaphthenequinonediimine (Mes-BIAN) has been attempted (for a complete list and details, see the Supporting Information). However, even a variation of the synthetic procedure did not allow us

 © 0000 Wiley-VCH Verlag GmbH & Co. KGaA, Weinheim

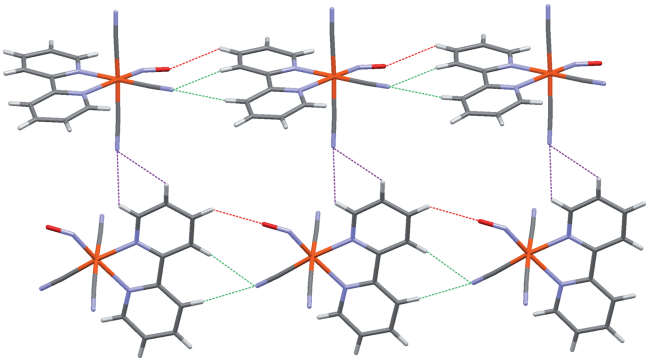

Figure 2. Hydrogen bonds in the $[Ph_4P][Fe(bpy)(CN)_3(NO)]$ structure C–H···O [red, intermolecular distance 2.558(2) Å] and C–H···N [green, intermolecular distances 2.558(2) and 2.588(2) Å] forming an infinite 1D arrangement. Interaction between chains through C–H···N contacts [purple, intermolecular distances 2.640(2) and 2.639(3) Å, respectively].

to isolate the corresponding complexes, with the exception of phen, which has been previously reported.[10,11]

Electrochemistry

The redox processes related to complex **1** were previously studied by polarography.[10,11] Thus, we explored its electrochemical behaviour by using cyclic voltammetry and also spectroelectrochemistry. To understand the influence of the diimine ligand we also studied the electrochemical behaviour of the 1,10-phenanthroline (phen) derivative, complex **2**, synthesised by a similar procedure to **1**. Both **1** and **2** display similar behaviour either in organic solvents or in aqueous media (Figure 3 and Figures S3 to S5 in the Supporting Information). For instance, in CH_2Cl_2, for complex **1** a reversible one-electron oxidation is observed at –0.31 V and additionally, two irreversible processes are detected at –1.83 and –2.42 V. Whereas the oxidation very probably

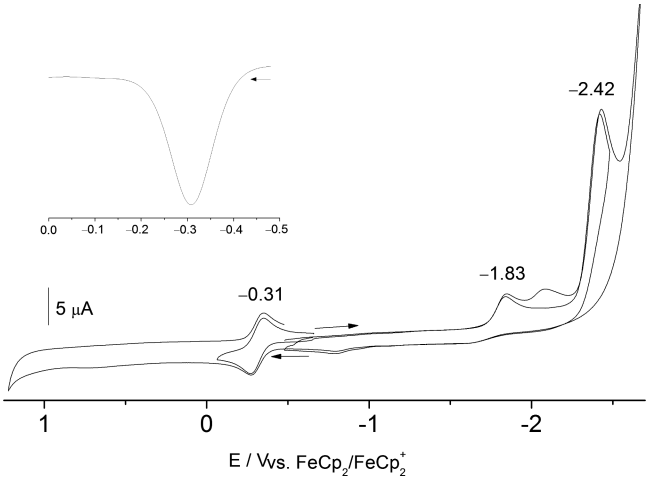

Figure 3. Cyclic voltammograms of $[Ph_4P][Fe(bpy)(CN)_3(NO)]$ in CH_2Cl_2/nBu_4NPF_6 at room temperature and 100 mV s^{-1} scan rate (bottom). Square-wave experiment of the reversible oxidation with 10 mV s^{-1} scan rate (top); both referenced against ferrocene/ferrocenium.

represents the $\{Fe(NO)\}^{7/6}$ couple, the reduction waves are probably due to bpy-based redox events coupled to loss of ligands (NO and/or CN). In the same solvent, for the phen complex **2**, the corresponding potentials are –0.29, –1.83 and –2.40 V (Table 1, Figure S5).

Table 1. Selected electrochemical data for $[Ph_4P][Fe(N^\wedge N)(CN)_3(NO)]$.[a]

	$E_{1/2}$ Ox1	E_{pc} Red1	E_{pc} Red2
$[Ph_4P][Fe(bpy)(CN)_3(NO)]$	–0.31	–1.83	–2.42
$[Ph_4P][Fe(phen)(CN)_3(NO)]$	–0.29	–1.83	–2.40

[a] Potentials in V versus ferrocene/ferrocenium from cyclic voltammetry or square-wave voltammetry in CH_2Cl_2/nBu_4PF_6 at 298 K and 100 mV s^{-1} scan rate. Half-wave potentials $E_{1/2}$ for the reversible oxidation, cathodic potential E_{pc} for irreversible reductions. Conversion to SCE = +0.46 V; to NHE = +0.66 V (see the literature as well[29]).

In MeCN solution a reversible oxidation is observed at –0.29 V for complex **1**, whereas a huge irreversible reduction wave lies at about –1.25 V (Figure S3 in the Supporting Information). In H_2O solution, for the values for complex **1**, the oxidation is shifted cathodically (–0.40 V versus ferrocene; 0.24 V versus SCE), whereas the reduction occurs at as low as –1.31 V versus ferrocene/ferrocenium (–0.91 V versus SCE; Figure S4; the measured SCE potentials were converted in to the ferrocene/ferrocenium scale by –0.643 V). The polarographically obtained potentials by Fiedler and Mašek are very similar to our values for the oxidation process[11] but differ largely for the reduction process, where they found far less negative potentials and the consumption of three electrons. Since parameters such as the electrode material, the scan rate, the concentration, temperature and solvent have a huge impact on the potential for irreversible processes, this is not unexpected. Similar problems have been observed for the determination of the first reduction potential of $[Fe(CN)_5(NO)]^{2-}$ from polarograms or cyclic voltammograms.[16] The first reduction of this complex ($\{Fe(NO)\}^{6\rightarrow7}$) is irreversible both in aqueous solution and in organic solvents owing to the loss of cyanide[16] and occurs at markedly more negative potentials [e.g., –0.82 V in CH_2Cl_2 (versus SCE)[16a]] than the oxidation of **1** ($\{Fe(NO)\}^{7\rightarrow6}$), thus the introduction of bpy or phen for two CN^- ligands has largely stabilised the $\{Fe(NO)\}^7$ complex.[10,11] Nevertheless, the potentials show that the complexes $[Fe(N^\wedge N)(CN)_3(NO)]^-$ can be easily oxidised, in line with their inherent instability during preparation and isolation. Furthermore, in line with the irreversible behaviour observed in the cyclic voltammograms, attempts to obtain the reduced $\{Fe(NO)\}^8$ (Fe^{II}–NO^-) complex by using cobaltocene or pentamethylcobaltocene were not successful.

UV/Vis Absorption Spectroelectrochemistry

The UV/Vis spectroelectrochemical anodic oxidation of compound **1** is shown in Figure 4. The long-wavelength bands of the starting complex with maxima at 381 and 449 nm, respectively, have been previously assigned to the ligand-to-metal charge-transfer band (LMCT; $NO^\cdot$ to

 © 0000 Wiley-VCH Verlag GmbH & Co. KGaA, Weinheim

Fe^{II}).[11] Alternatively, these bands might be assigned to metal(Fe^{II})-to-ligand (π*,bpy) transitions as observed in $[Fe(bpy)(CN)_4]^{2-}$.[30] In addition to these bands, a weak shoulder at 550 nm is discernible that is probably due to d–d transitions.[3d,11,30] Intraligand π–π* bands were observed at 233 and 294 nm, respectively.[11] The tiny features at around 270 nm are due to the counterion. Upon anodic oxidation, the long-wavelength bands vanish and only very weak long-wavelength absorptions at 460 and 550 nm remain, the intensity of the 233 nm intraligand band is diminished and the 294 nm band undergoes a redshift to yield a band with maxima at 302 and 312 nm. Isosbestic points are observed at 305 and 338 nm.

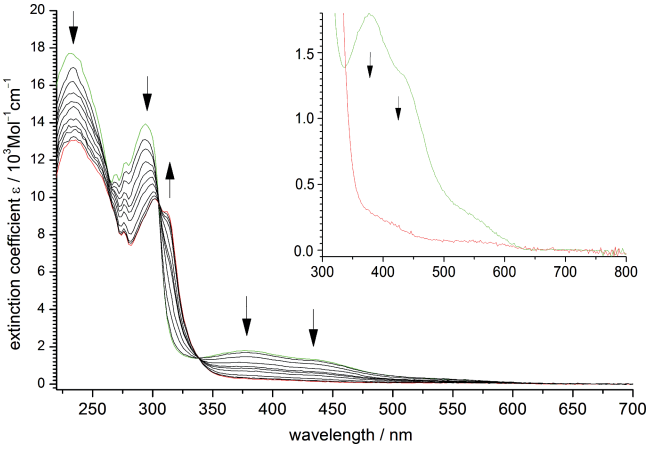

Figure 4. UV/Vis absorption spectra recorded during reversible anodic oxidation of $[Ph_4P][Fe(bpy)(CN)_3(NO)]$ in CH_2Cl_2/$n$$Bu_4NPF_6$ at room temperature in an optically transparent thin-layer electrode (OTTLE) cell (applied potential 0–800 mV). Inset: Parent complex in green and product of the oxidation in red.

The oxidation occurs completely reversibly on the timescale of the experiment. Re-reduction after anodic sweep produced more than 97% of the original spectral intensity. The product of the oxidation $[Fe(bpy)(CN)_3(NO)]$ [{Fe(NO)}^{6}] exhibits very weak long-wavelength bands around 500 nm (see inset in Figure 4), which we tentatively assign to d–d transitions[3c,3d,11] and redshifted intense π–π* absorption bands. Both features are in line with a low-spin Fe^{II} and NO^+ description as already assumed by Fiedler and Mašek.[10,11] The metal-to-ligand charge-transfer band (MLCT; Fe^{II} to NO^+), which occurs in the visible range for $[Fe(CN)_5(NO)]^{2-}$[3c,8a] seems to be shifted to the UV range in $[Fe(bpy)(CN)_3(NO)]$ owing to the weaker ligand bpy (compared with $2 \times CN^-$) and the reduced charge of the complex, and is probably hidden under the intense π–π* absorption bands.

Thus, our UV/Vis spectroelectrochemical experiment strongly supports the LMCT assignment for the long-wavelength bands of the parent complex **1** and the d–d character of the very long-wavelength shoulder. The possible MLCT (Fe^{II}-to-π*,bpy) transitions that occur in the visible region for $[Fe(bpy)(CN)_4]^{2-}$[30] were not observed for **1** in the visible and might be hidden under the intense π–π* absorption bands. In $[Fe(bpy)_2(CN)_2]$, as in $[Fe(bpy)_3]^{2+}$, the d–d excited state lies also lower than this MLCT,[30,31] which means that two CN^- ligands (for one bpy) are not enough to increase the d–d energy and lower the MLCT energy, whereas four CN^- ligands as in $[Fe(bpy)(CN)_4]^{2-}$ seem to be sufficient for this task. Starting from this complex, the formal replacement of CN^- by $NO^{\cdot}$ in $[Fe(bpy)(CN)_3(NO)]^-$ results in a weaker ligand field, reduced charge of the complex and lower electron density in the Fe^{II}, which shifts this MLCT to higher energy.

EPR Spectroscopy and Electronic Structure Calculations

X-band (9.4 GHz) EPR spectra were recorded on solid samples and solutions of **1** in CH_2Cl_2 (Figure 5 and Figure S7 in the Supporting Information).

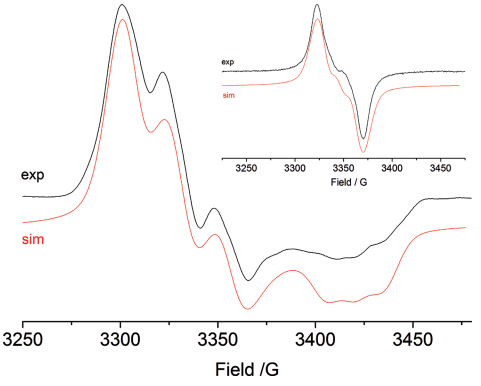

Figure 5. X-band EPR spectra of $[Ph_4P][Fe(bpy)(CN)_3(NO)]$ in glassy frozen CH_2Cl_2 (conc. approx. 10^{-5} mol L^{-1}) at 110 K and at room temperature (inset) with simulations.

Whereas in a solution in CH_2Cl_2 an ill-resolved isotropic spectrum at g = 2.0107 is observed (Figure 5, inset), the anisotropic spectrum recorded at 110 K in glassy frozen solution (Figure 5) can be simulated by assuming a rhombic symmetry with three g values (g_1 = 2.035, g_2 = 2.025, g_3 = 1.972) and hyperfine splitting for one N nucleus (I = 1) for the NO ligand (A_1 = 11 G, A_2 = 25 G, A_3 = 15 G; line width 18, 15, and 14 G, Lorentzian/Gaussian: 0.9), which is in line with an $S = {}^1/_2$ system that represents a diamagnetic Fe^{II}, low-spin system and the unpaired electron largely localised on the NO ligand. With this data, the isotropic spectrum at room temperature (Figure 5, inset) could be also simulated, and interestingly, the simulation was slightly better when assuming two different N-atom contributions to the unpaired electron with $A_{iso(NO)}$ = 16 G and $A_{iso(Nbpy\ trans\ to\ NO)}$ = 2 G (line width 17.5 G).

Thus, the EPR results confirm the assumption of Fiedler and Mašek that the observed magnetic moment (μ_{eff}) for $[Ph_4P][Fe(bpy)(CN)_3(NO)]$ of 2.27 B.M. is higher than the spin-only value of 1.73 B.M. owing to orbital contribution and not to a higher-spin system.[11] For the complexes $[Fe(CN)_5(NO)]^{3-}$ and $[Fe(CN)_4(NO)]^{2-}$ the magnetic moment has been determined to be 1.73 B.M. with no orbital contribution.[15] From our results we can say that the spin is largely localised on the NO ligand; however, the high isotropic g value and the g anisotropy ($\Delta g = g_1 - g_3$) in the

 © 0000 Wiley-VCH Verlag GmbH & Co. KGaA, Weinheim

spectrum at 110 K of 0.063 point to a marked contribution of the iron atom. For $[Fe(CN)_5(NO)]^{3-}$ an axial spectrum with $g_1 = g_2 = 1.99$, $g_3 = 1.92$ with an averaged g value $g_{avg.}$ below 2, $\Delta g = 0.07$ and $A_2 = 28$ G has been reported.[3c,12a] Parameters very similar to the values observed for $[Fe(bpy)(CN)_3(NO)]^-$ were reported for $[Fe(pyN_4)(NO)]^{2+}$ {PyN_4 = 2,6-$C_5H_3N[CMe(CH_2NH_2)_2]_2$} ($g_{avg.}$ = 2.007, Δg = 0.085)[17] and the two forms of the complex $[Fe(cyclam\text{-}ac)(NO)]^+$ (cyclam-acH = 1,4,8,11-tetraazacyclotetradecane-1-acetic acid) with $g_{avg.}$ of 2.014 and 2.012 and Δg = 0.065 and 0.088, respectively.[22a] For the last system, the structural parameters ∠FeNO ≈ 148° and *d*NO = 1.166(6) Å are in complete agreement with the parameters for $[Fe(bpy)(CN)_3(NO)]^-$, which points to the fact that the Fe(NO) fragment largely dominates the spin distribution in these {Fe(NO)}^{7} systems. Also for the complex $[Fe(PaPy_3)(NO)]^+$ {$PaPy_3H$ = *N*,*N*-bis(2-pyridylmethyl)amine-*N*-ethyl-2-pyridine-2-carboxamide} a markedly lower $g_{avg.}$ of 1.989 is in line with a slightly changed Fe(NO) geometry [∠FeNO = 141.3(2)° and *d*NO = 1.190(2) Å], whereas the Δg of 0.088 is similar.[19] In all the aforementioned systems a large A_2 value of more than 25 G is also a common feature. Very recently, Solomon, Jameson, Goldberg et al. reported on two structurally related complexes, $[Fe(N_3PyS)(NO)]^+$ and $[Fe(N_4Py)(NO)]^{2+}$ {N_3PySH = *N*-[2-phenylthiolmethyl-*N*-(2-pyridinylmethyl-*N*,*N*-bis(2-pyridinylmethyl)methylamine; N_4Py = 1,1-di(2-pyridinyl)-*N*,*N*-bis(2-pyridinylmethyl)methanamine)]}, with quite different $g_{avg.}$ values of 2.005 for N_3PyS and 1.996 for N_4Py but a virtually identical Δg value of 0.085.[21] The A_2 value for the N_3PyS complex is markedly lower (21.1 G) than for the N_4Py derivative (25.1 G). Also here, the Fe(NO) geometry seems to be crucial. Whereas the N_3PyS complex exhibits ∠FeNO = 147.2(2)° and *d*NO = 1.150(3) Å, the N_4Py derivative has ∠FeNO = 144.9(2)° and *d*NO = 1.157(3) Å.

A broad overview of various {Fe(NO)}^{7} systems is provided in Table S3 of the Supporting Information. From this we can conclude that the averaged g value ($g_{avg.}$) is quite sensitive to the Fe(NO) geometry with higher values for large angles. The A_2 coupling constant and the g anisotropy (Δg) is quite constant for most six-coordinate ferrous nitrosyl {Fe(NO)}^{7} systems; smaller values were observed for five-coordinate systems,[23e,24b] whereas slightly larger Δg values for six-coordinate systems were observed for porphyrin-based systems.[23d] However, a conclusive correlation of Fe(NO) structural data and EPR parameters is lacking because the structural data has been achieved in the crystal, whereas EPR data is recorded in glassy frozen solution. Additionally, more examples of such low-spin {Fe(NO)}^{7} systems would be welcome.

In recent literature, it was shown for $[Fe(NO)]^{2+}$, as a model for the {Fe(NO)}^{7} complexes,[32] that among the tested exchange-correlation functionals none of them is able enough to provide a satisfactory description of the spin densities relative to complete active space self-consistent field (CASSCF) calculations. However, for complex **1** the results obtained from DFT calculations under vacuum are in good agreement with the EPR results. The relative spin-state energies obtained for the $[Fe(bpy)(CN)_3(NO)]^-$ anion (Table S4 in the Supporting Information) using different functionals (see the Experimental Section for details) showed that the singlet state is favoured in all cases with respect to the triplet state with stabilisation energies in the range of 23.1–27.8 kcal mol^{-1}. In addition, a similar spin-density distribution that satisfactorily describes our system is observed for the singlet state for the tested functionals (Figure S8). As expected, in all cases the calculated spin densities are centred among the Fe(NO) moiety, but no significant differences were found for the different applied functionals, contrary to what has been observed for similar systems.[32]

EPR and IR Spectroelectrochemistry

Additionally, we investigated the EPR response to the anodic oxidation of **1** in $CH_2Cl_2/n Bu_4NPF_6$ at room temperature (Figure 6). Upon oxidation, the isotropic signal at g = 2.0107 completely disappeared and reappeared upon re-reduction. The EPR silence of the oxidised product $[Fe(bpy)(CN)_3(NO)]$ could be either due to a ferromagnetically coupled low-spin Fe^{III} and $NO^{\cdot}$ or to diamagnetic low-spin Fe^{II} and diamagnetic NO^+. From spectroelectro-IR experiments (Figure S9 in the Supporting Information) in which the νNO band shifts from 1660 to 1930 cm^{-1} and the νCN bands shifts from 2108 to 2142 cm^{-1} upon oxidation, we conclude that the latter description of an Fe^{II}–NO^+ complex is far more appropriate, in line with the conclusions from UV/Vis spectroelectrochemistry and the assumptions by Fiedler and Mašek.[11] On the timescale of the IR and EPR spectroelectrochemical experiments, the oxidation of the complex **1** is reversible.

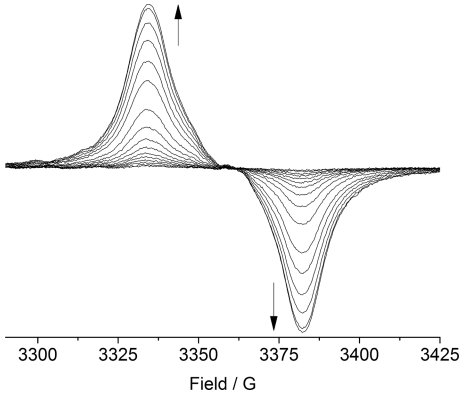

Figure 6. X-band EPR spectra recorded during re-reduction of anodically oxidised $[Ph_4P][Fe(bpy)(CN)_3(NO)]$ in $CH_2Cl_2/n Bu_4NPF_6$ at room temperature (ox: –0.6→+2.0 V; re-red: +2.0→–0.6 V/0.2 V steps). The arrows indicate the signal growth upon re-reduction.

Upon cathodic reduction of **1**, the EPR signal vanishes. In the IR, the νNO band at 1660 cm^{-1} intensifies, whereas the νCN band shifts to 2086 cm^{-1}. Importantly, the reduction is completely irreversible.

 © 0000 Wiley-VCH Verlag GmbH & Co. KGaA, Weinheim

Conclusion

The $\{Fe(NO)\}^7$ complex $[PPh_4][Fe(bpy)(CN)_3(NO)]$ has been fully characterised. Its molecular structure (from single-crystal XRD) shows a bent nitrosyl, and EPR data and DFT calculations confirm that its electronic configuration involves a diamagnetic low-spin Fe^{II} with the unpaired electron density localised on the $NO^{\cdot}$ ligand. The brownish red colour of the complex is due to long-wavelength LMCT ($NO^{\cdot}$ to Fe^{II}) absorptions, and the complex can be reversibly oxidised to the $\{Fe(NO)\}^6$ (Fe^{II}–NO^+) complex, as confirmed by UV/Vis, EPR and IR spectroelectrochemistry. Attempts to obtain the reduced $\{Fe(NO)\}^8$ (Fe^{II}–NO^-) complex by using chemical reductants failed, probably due to the irreversible character of this reduction, as observed in the CV and spectroelectrochemical experiments. Moreover, the $NO^{\cdot}$ ligand in the parent $\{Fe(NO)\}^7$ complex seems to be highly sensitive to the environment, since replacement of bipyridine with other ligands with similar properties, such as phenanthroline, produced complexes that were much more reactive or were not formed at all.

Experimental Section

General: All syntheses and manipulations were carried out under strictly controlled atmospheres of nitrogen or argon.

Instrumentation: EPR spectra were recorded in the X-band with a Bruker ELEXSYS500E equipped with a Bruker variable-temperature unit ER 4131VT (500 to 100 K); *g* values were determined using a 2,2-diphenyl-1-picrylhydrazyl (dpph) sample. UV/Vis absorption spectra were measured with a Varian Cary 05E/Varian Cary50 Scan photospectrometer. Spectroelectrochemical investigations (UV/Vis and IR) were performed at ambient temperature with an OTTLE cell.[33] EPR spectroelectrochemistry was performed in an EPR tube equipped with three electrodes (working E: Pt; counter-E: Pt and pseudo-reference-E: Ag). IR spectra were recorded with a Nicolet Avatar 320 FTIR spectrometer with a Spectra Tech cell for KBr pellets. Electrochemical experiments were carried out in 0.1 M nBu_4NPF_6 solutions using a three-electrode configuration (glassy carbon electrode, Pt counter electrode, Ag/AgCl reference) and an Autolab PGSTAT30 potentiostat and function generator. Data were processed using GPES 4.9 (General Electrochemical System Version 4.9). The ferrocene/ferrocenium couple ($FeCp_2$/$FeCp_2^+$) served as internal reference.

General Procedure for the Preparation of $[Ph_4P][Fe(N^\wedge N)(CN)_3(NO)]$ complexes (N^N = bpy, phen): Sodium nitroprusside (1 mmol, 298 mg) was dissolved in nitrogen-purged water (40 mL). Afterwards sodium dithionite (2 mmol, 350 mg, 2 equiv.) was added in water (10 mL), followed by the addition of the N^N ligand (1 equiv.; 156 mg of bpy, 180 mg of phen). The solution was stirred for three hours, and the colour changed from greenish to dark brown. A solution of tetraphenylphosphonium bromide (1 mmol, 420 mg) in water (20 mL) was added to the mixture and stirring was continued for one hour. The mixture was left overnight under an inert atmosphere to complete the precipitation. The mixture was filtered and the brown residue was washed with water (3 × 20 mL). The crude product was dissolved in degassed ethanol and recrystallised by adding diethyl ether. The mixture was centrifuged and the solvent was removed under reduced pressure to obtain a microcrystalline brownish red solid. Compound **1** (bpy) yield: 47%. $C_{37}H_{38}FeN_6OP$ (659.48): calcd. C 67.39, H 4.28, N 12.74; found C 67.42, H 4.25, N 12.77. IR (KBr): ν_{NO} = 1642 cm^{-1}, ν_{CN} 2108 cm^{-1}. Compound **2** (phen) yield: 35%. $C_{39}H_{28}FeN_6OP$ (683.50): calcd. C 68.53, H 4.13, N 12.30; found C 68.25, H 4.11, N 12.33. IR (KBr): ν_{NO} 1641 cm^{-1}, ν_{CN} 2106 cm^{-1}.

X-ray Diffraction: The structure of **1** was solved by means of direct methods[34] and refined by full-matrix least-squares[35] on F^2. X-ray reflections were collected at 298 K with an Oxford Xcalibur Gemini Eos CCD diffractometer using Mo-K_α radiation (λ = 0.7107 Å). Data collection and processing, including a multiscan absorption correction were performed using CrysAlisPro (version 1.171.33.55),[36] and OLEX2–1.2[37] and SHELXL97[38] were used for structure solution and refinement. In the course of the refinement, several hydrogen atoms were detected at approximate locations in difference Fourier maps and then refined freely. Several reflections were flagged as having an extremely poor match of $F_{obsd.}$ to $F_{calcd.}$, probably owing to beamstop interference. The omission of those reflections does not introduce any modification in the refinement parameters.

CCDC-1026302 (for **1**) contains the supplementary crystallographic data for this paper. These data can be obtained free of charge from The Cambridge Crystallographic Data Centre via www.ccdc.cam.ac.uk/data_request/cif.

Computational Methodology: All unrestricted Kohn–Sham DFT calculations were performed with the Gaussian 09 quantum chemical program.[39] Six popular exchange-correlation functionals were employed: B3LYP,[40] OLYP,[41] OPB,[42] BP86,[43] BLYP[44] and M06-L.[45] For direct comparison, all DFT spin-density profiles were obtained from single-point calculations on the optimised structure. We applied the 6-31G** basis set in all cases.[46] The spin-density distributions were visualised using the Gabedit 2.4 program (Figure S8 in the Supporting Information).[47]

Supporting Information (see footnote on the first page of this article): Figures showing cyclic voltammograms of complexes **1** and **2**; UV/Vis absorption and IR spectra of **2**; IR spectroelectrochemistry of **1**; an EPR spectrum (in the solid) of **1**; and calculated spin-density profiles for complex **1** are provided together with tables that contain structural information and EPR data for selected $\{Fe(NO)\}^7$ complexes and details on further attempted complex syntheses.

Acknowledgments

This work was financially supported by Deutscher Akademischer Austauschdienst–Ministerio Nacional de Ciencia y Tecnologia (DAAD-MINCyT) (grant number 50752227), by the Deutsche Forschungsgemeinschaft (DFG)–Consejo Nacional de Investigaciones Cientificas y Tecnicas (CONICET) (COOPINT DFG-CONICET) (grant to A. K.); the DFG projects KL1194/12-1 and KL1194/13-1; project D978, MINCyT, PICT 2010-2549 (grant to F. D.); and by the Third World Academy of Sciences (TWAS). A. F. acknowledges the Universidad de Buenos Aires (UBA) for her scholarships.

[1] a) F. Doctorivich, P. J. Farmer, *J. Inorg. Biochem.* **2013**, *118*, 107; b) A. de Mel, F. Murad, A. M. Seifalian, *Chem. Rev.* **2011**, *111*, 5742–5767; c) B. G. Hill, B. P. Dranka, S. M. Bailey, J. R. Lancaster Jr., V. M. Darley-Usmar, *J. Biol. Chem.* **2010**, *285*, 19699–19704; d) Z. J. Tonzetich, L. E. McQuade, S. J. Lippard, *Inorg. Chem.* **2010**, *49*, 6338–6348; e) A. R. Butler, I. L. Megson, *Chem. Rev.* **2002**, *102*, 1155–1165.

[2] a) A. L. Speelman, N. Lehnert, *Acc. Chem. Res.* **2014**, *47*, 1106–1116; b) A. Franke, R. van Eldik, *Eur. J. Inorg. Chem.*

 © 0000 Wiley-VCH Verlag GmbH & Co. KGaA, Weinheim

2013, 460–480; c) H. Lewandowska, M. Kalinowska, K. Brzoska, K. Wojciuk, G. Wojciuk, M. Kruszewski, *Dalton Trans.* **2011**, *40*, 8273–8289; d) P. C. Ford, *Inorg. Chem.* **2010**, *49*, 6226–6239; e) G. B. Richter-Addo, P. Legzdins, J. Burtyn, *Chem. Rev.* **2002**, *102*, 857–859.

[3] a) J. Pellegrino, R. Hübner, F. Doctorovich, W. Kaim, *Chem. Eur. J.* **2011**, *17*, 7868–7874; b) J. A. Olabe, *Physical Inorganic Chemistry: Reactions, Processes, and Applications*, Wiley, Hoboken, N.J., USA, **2010**; c) J. A. Olabe, *Dalton Trans.* **2008**, 3633–3648; d) F. Roncaroli, M. Videla, L. D. Slep, J. A. Olabe, *Coord. Chem. Rev.* **2007**, *251*, 1903–1930; e) M. C. Gonzales Lebrero, D. A. Scherlis, G. L. Estiu, J. A. Olabe, D. A. Estrin, *Inorg. Chem.* **2001**, *40*, 4127–4133.

[4] a) T. Xu, N. Scafa, L.-P. Xu, L. Su, C. Li, S. Zhou, Y. Liu, X. Zhang, *Electroanalysis* **2014**, *26*, 449–468; b) N. Xu, L. Goodrich, N. Lehnert, D. R. Powell, G. B. Richter-Addo, *Angew. Chem. Int. Ed.* **2013**, *52*, 3896–3900; *Angew. Chem.* **2013**, *125*, 3988; c) P. Wu, J. Wang, C. He, X. Zhang, Y. Wang, T. Liu, *Adv. Funct. Mater.* **2012**, *22*, 1698–1703; d) N. Xu, J. Yi, G. B. Richter-Addo, *Inorg. Chem.* **2010**, *49*, 6253–6266; e) U. Schatzschneider, *Eur. J. Inorg. Chem.* **2010**, 1451–1467.

[5] A. R. Butler, C. Glidewell, *Chem. Soc. Rev.* **1987**, *16*, 361–380.

[6] a) A. C. Montenegro, S. E. Bari, J. A. Olabe, *J. Inorg. Biochem.* **2013**, *118*, 108–114; b) A. C. Montenegro, S. G. Dabrowski, M. M. Gutierrez, W. T. Amorebieta, S. E. Bari, J. A. Olabe, *Inorg. Chim. Acta* **2011**, *374*, 447–452; c) A. C. Montenegro, V. T. Amorebieta, L. D. Slep, D. F. Martin, F. Roncaroli, D. H. Murgida, S. E. Bari, J. A. Olabe, *Angew. Chem. Int. Ed.* **2009**, *48*, 4213–4216; *Angew. Chem.* **2009**, *121*, 4277.

[7] a) M. M. Gutierrez, J. A. Olabe, V. T. Amorebieta, *Eur. J. Inorg. Chem.* **2012**, 4433–4438; b) S. L. Quiroga, A. E. Almaraz, V. T. Amorebieta, L. L. Perissinotti, J. A. Olabe, *Chem. Eur. J.* **2011**, *17*, 4145–4156; c) M. M. Gutierrez, G. B. Alluisetti, J. A. Olabe, V. T. Amorebieta, *Dalton Trans.* **2008**, 5025–5030; d) C. Trapani, N. Escola, F. Doctorovich, *Organometallics* **2002**, *21*, 2021–2023; e) F. Doctorovich, N. Escola, C. Trapani, D. A. Estrin, M. C. Gonzales Lebrero, A. G. Turjanski, *Organometallics* **2000**, *19*, 3810–3817.

[8] a) D. A. Estrin, L. M. Baraldo, L. D. Slep, B. C. Barja, A. A. Olabe, L. Paglieri, G. Corongiu, *Inorg. Chem.* **1996**, *35*, 3897–3903; b) D. F. Watson, A. B. Bocarsly, *Coord. Chem. Rev.* **2001**, *211*, 177–194.

[9] a) R. Herchel, Z. Travnicek, R. Zboril, *Inorg. Chem.* **2011**, *50*, 12390–12392; b) L. M. Baraldo, P. Forlano, A. R. Parise, L. D. Slep, J. A. Olabe, *Coord. Chem. Rev.* **2001**, *219–221*, 881–921.

[10] J. Fiedler, J. Mašek, *Inorg. Chim. Acta* **1984**, *81*, 117–120.

[11] J. Fiedler, J. Mašek, *Inorg. Chim. Acta* **1985**, *105*, 83–87.

[12] a) M. Wanner, T. Scheiring, W. Kaim, L. D. Slep, L. M. Baraldo, J. A. Olabe, S. Zalis, E. J. Baerends, *Inorg. Chem.* **2001**, *40*, 5704–5707; b) F. Baumann, W. Kaim, L. M. Baraldo, L. D. Slep, J. A. Olabe, J. Fiedler, *Inorg. Chim. Acta* **1999**, *285*, 129–133.

[13] a) L. L. Perissinotti, D. A. Estrin, G. Leitus, F. Doctorovich, *J. Am. Chem. Soc.* **2006**, *128*, 2512–2513; b) M. Sieger, B. Sarkar, S. Zalis, J. Fiedler, N. Escola, F. Doctorovich, J. A. Olabe, W. Kaim, *Dalton Trans.* **2004**, 1797–1800; c) S. Frantz, B. Sarkar, M. Sieger, W. Kaim, F. Roncaroli, J. A. Olabe, S. Zalis, *Eur. J. Inorg. Chem.* **2004**, 2902–2907.

[14] J. H. Enemark, R. D. Feltham, *Coord. Chem. Rev.* **1974**, *13*, 0–406.

[15] R. Nast, J. Schmidt, *Z. Anorg. Allg. Chem.* **1976**, *421*, 15–23.

[16] a) W. L. Bowden, P. Bonnar, D. B. Brown, W. E. Geiger, *Inorg. Chem.* **1977**, *16*, 41–43; b) J. Masek, E. Maslova, *Collect. Czech. Chem. Commun.* **1974**, *39*, 2141–2161.

[17] J. P. Lopez, F. W. Heinemann, R. Prakash, B. A. Hess, O. Horner, C. Jeandy, J.-L. Oddou, J.-M. Latour, A. Grohmann, *Chem. Eur. J.* **2002**, *8*, 5709–5722.

[18] D. Sellmann, N. Blum, F. W. Heinemann, B. A. Hess, *Chem. Eur. J.* **2001**, *7*, 1874–1880.

[19] A. K. Patra, J. M. Rowland, D. S. Marlin, E. Bill, M. M. Olmstead, P. K. Mascharak, *Inorg. Chem.* **2003**, *42*, 6812–6823.

[20] Y. Chen, M. A. Sweetland, R. E. Shepherd, *Inorg. Chim. Acta* **1997**, *260*, 163–172.

[21] A. C. McQuilken, Y. Ha, K. D. Sutherlin, M. A. Siegler, K. O. Hodgson, B. Hedman, E. I. Solomon, G. N. L. Jameson, D. P. Goldberg, *J. Am. Chem. Soc.* **2013**, *135*, 14024–14027.

[22] a) R. Garcia Serres, C. A. Grapperhaus, E. Bothe, E. Bill, T. Weyhermüller, F. Neese, K. Wieghardt, *J. Am. Chem. Soc.* **2004**, *126*, 5138–5153; b) C. Hauser, T. Glaser, E. Bill, T. Weyhermüller, K. Wieghardt, *J. Am. Chem. Soc.* **2000**, *122*, 4352–4365.

[23] Examples of low-spin (S = 1/2) Fe^{II}–$NO^{\cdot}$ = $\{Fe(NO)\}^7$ systems are described in ref.[15–21a], see also: a) N. Xu, D. R. Powell, G. B. Richter-Addo, *Nitric Oxide* **2014**, *37*, 61–65; b) P. Surawatanawong, S. Sproules, F. Neese, K. Wieghardt, *Inorg. Chem.* **2011**, *50*, 12064–12074; c) M. Radon, E. Broclawik, K. Pierloot, *J. Phys. Chem. B* **2010**, *114*, 1518–1528; d) T. C. Berto, V. K. K. Praneeth, L. E. Goodrich, N. Lehnert, *J. Am. Chem. Soc.* **2009**, *131*, 17116–17126; e) P. Ghosh, K. Stobie, E. Bill, E. Bothe, T. Weyhermüller, M. D. Ward, J. A. McCleverty, K. Wieghardt, *Inorg. Chem.* **2007**, *46*, 522–532; f) R. K. Afhar, A. K. Patra, E. Bill, M. M. Olmstead, P. K. Mascharak, *Inorg. Chem.* **2006**, *45*, 3774–3781; g) T. C. Harrop, M. M. Olmstead, P. K. Mascharak, *Inorg. Chem.* **2005**, *44*, 6918–6920; h) C.-Y. Chiang, J. Lee, C. Dalrymple, M. C. Sarahan, J. H. Reibenspies, M. Y. Darensbourg, *Inorg. Chem.* **2005**, *44*, 9007–9016; i) H. Nasri, M. K. Ellison, S. Chen, B. H. Huynh, W. R. Scheidt, *J. Am. Chem. Soc.* **1997**, *119*, 6274–6283.

[24] Alternatively, (S = 1/2) $\{Fe(NO)\}^7$ systems have been described as Fe^{I}–NO^{+}, for examples see: a) B. C. Sanders, A. K. Patra, T. C. Harrop, *J. Inorg. Biochem.* **2013**, *118*, 115–127; b) I.-J. Hsu, C.-H. Hsieh, S.-C. Ke, K.-A. Chiang, J.-M. Lee, J.-M. Chen, L.-Y. Jang, G.-H. Lee, Y. Wang, W.-F. Liaw, *J. Am. Chem. Soc.* **2007**, *129*, 1151–1159.

[25] For examples of high-spin (S = 3/2) Fe^{II}–$NO^{\cdot}$ = $\{FeNO\}^7$ see: a) J. Li, A. Banerjee, P. L. Pawlak, W. W. Brennessel, F. A. Chavez, *Inorg. Chem.* **2014**, *53*, 5414–5416; b) S. Chakraborty, J. Reed, M. Ross, M. J. Nilges, I. D. Petrik, S. Ghosh, S. Hammes-Schiffer, J. T. Sage, Y. Zhang, C. E. Schulz, Y. Lu, *Angew. Chem. Int. Ed.* **2014**, *53*, 2417–2421; c) A. L. Speelman, N. Lehnert, *Angew. Chem. Int. Ed.* **2013**, *52*, 12283–12287; *Angew. Chem.* **2013**, *125*, 12509; d) J. Conradie, K. H. Hopmann, A. Ghosh, *J. Phys. Chem. B* **2010**, *114*, 8517–8524; e) F. Aquino, J. H. Rodriguez, *J. Phys. Chem. A* **2009**, *113*, 9159–9156; f) A. Wanat, T. Schneppensieper, G. Stochel, R. van Eldik, E. Bill, K. Wieghardt, *Inorg. Chem.* **2002**, *41*, 4–10; g) M. Ray, A. P. Golombek, M. P. Hendrich, G. P. A. Yap, L. M. Liable-Sands, A. L. Rheingold, A. S. Borovik, *Inorg. Chem.* **1999**, *38*, 3110–3115; h) C. A. Brown, M. A. Pavlosky, T. E. Westre, Y. Zhang, B. Hedman, K. O. Hodgson, E. I. Solomon, *J. Am. Chem. Soc.* **1995**, *117*, 715–732; i) K. Pohl, K. Wieghardt, B. Nuber, J. Weiss, *J. Chem. Soc., Dalton Trans.* **1987**, 187–192.

[26] For examples of Fe^{II}–$NO^{\cdot}$ = $\{Fe(NO)\}^7$ systems with spin equilibria S = 1/2–3/2 or mixed-spin systems see ref.[3c,21b] and also: a) M. Li, D. Bonnet, E. Bill, F. Neese, T. Weyhermüller, N. Blum, D. Sellmann, K. Wieghardt, *Inorg. Chem.* **2002**, *41*, 3444–3456; b) M. S. Ward, R. E. Shepherd, *Inorg. Chim. Acta* **1999**, *286*, 197–206; c) F. V. Wells, S. W. McCann, H. H. Wickman, S. L. Kessel, D. N. Hendrickson, R. D. Feltham, *Inorg. Chem.* **1982**, *21*, 2306–2311.

[27] a) L. Cheng, G. B. Richter-Addo, in: *The Porphyrin Handbook* (Eds.: R. Guilard, K. Smith, K. M. Kadish), vol. 4, Academic Press, New York, **2000**, p. 219–291; b) G. B. Richter-Addo, P. Legdzins, in: *Metal Nitrosyls*, Oxford University Press, New York, **1992**.

[28] J. Conradie, A. Ghosh, *Inorg. Chem.* **2011**, *50*, 4223–4225.

[29] N. G. Connelly, W. E. Geiger, *Chem. Rev.* **1996**, *96*, 877–910.

[30] J. R. Winkler, C. Creutz, N. Sutin, *J. Am. Chem. Soc.* **1987**, *109*, 3471–3472.

 © 0000 Wiley-VCH Verlag GmbH & Co. KGaA, Weinheim

[31] J. R. Winkler, N. Sutin, *Inorg. Chem.* **1987**, *26*, 220–221.
[32] K. Boguslawski, C. R. Jacob, M. Reiher, *J. Chem. Theory Comput.* **2011**, *7*, 2740–2752.
[33] a) W. Kaim, J. Fiedler, *Chem. Soc. Rev.* **2009**, *38*, 3373–3382; b) M. Krejčík, M. Daňek, F. Hartl, *J. Electroanal. Chem.* **1991**, *317*, 179–187.
[34] G. M. Sheldrick, *SHELX97*, *Programs for Crystal Structure Analysis*, release 97–2, University of Göttingen, Germany, **1998**.
[35] J. Bruno, J. C. Cole, P. R. Edgington, M. Kessler, C. F. Macrae, P. McCabe, J. Pearson, R. Taylor, *Acta Crystallogr., Sect. B* **2002**, *58*, 389–397.
[36] *CrysAlis CCD* and *CrysAlis RED*, versions 1.171.33.55, Oxford Diffraction Ltd., Yarnton, Oxfordshire, UK, **2011**.
[37] O. B. Dolomanov, A. J. Blake, N. R. Champness, M. J. Schröder, *J. Appl. Crystallogr.* **2003**, *36*, 1283–1284.
[38] G. M. Sheldrick, *SHELXS-97* and S*HELXL-97*, University of Göttingen, Germany, **1997**.
[39] M. J. Frisch, G. W. Trucks, H. B. Schlegel, G. E. Scuseria, M. A. Robb, J. R. Cheeseman, G. Scalmani, V. Barone, B. Mennucci, G. A. Petersson, H. Nakatsuji, M. Caricato, X. Li, H. P. Hratchian, A. F. Izmaylov, J. Bloino, G. Zheng, J. L. Sonnenberg, M. Hada, M. Ehara, K. Toyota, R. Fukuda, J. Hasegawa, M. Ishida, T. Nakajima, Y. Honda, O. Kitao, H. Nakai, T. Vreven, J. A. Montgomery Jr., J. E. Peralta, F. Ogliaro, M. Bearpark, J. J. Heyd, E. Brothers, K. N. Kudin, V. N. Staroverov, R. Kobayashi, J. Normand, K. Raghavachari, A. Rendell, J. C. Burant, S. S. Iyengar, J. Tomasi, M. Cossi, N. Rega, J. M. Millam, M. Klene, J. E. Knox, J. B. Cross, V. Bakken, C. Adamo, J. Jaramillo, R. Gomperts, R. E. Stratmann, O. Yazyev, A. J. Austin, R. Cammi, C. Pomelli, J. W. Ochterski, R. L. Martin, K. Morokuma, V. G. Zakrzewski, G. A. Voth, P. Salvador, J. J. Dannenberg, S. Dapprich, A. D. Daniels, O. Farkas, J. B. Foresman, J. V. Ortiz, J. Cioslowski, D. J. Fox, *Gaussian 09*, revision D.01, Gaussian, Inc., Wallingford CT, **2009**.
[40] A. D. Becke, *J. Chem. Phys.* **1993**, *98*, 5648–5652.
[41] a) J. P. Perdew, K. Burke, M. Ernzerhof, *Phys. Rev. Lett.* **1996**, *77*, 3865–3868; b) J. P. Perdew, K. Burke, M. Ernzerhof, *Phys. Rev. Lett.* **1997**, *78*, 1396–1396.
[42] a) A. D. Becke, *Phys. Rev. A* **1988**, *38*, 3098–3100; b) J. P. Perdew, *Phys. Rev. B* **1986**, *33*, 8822–8824.
[43] C. Lee, W. Yang, R. G. Parr, *Phys. Rev. B* **1988**, *37*, 785–789.
[44] Y. Zhao, D. G. Truhlar, *J. Chem. Phys.* **2006**, *125*, 194101–194118.
[45] V. A. Rassolov, J. A. Pople, M. A. Ratner, T. L. Windus, *J. Chem. Phys.* **1998**, *109*, 1223–1229.
[46] a) M. M. Francl, W. J. Pietro, W. J. Hehre, J. S. Binkley, D. J. DeFrees, J. A. Pople, M. S. Gordon, *J. Chem. Phys.* **1982**, *77*, 3654–3665; b) V. Rassolov, J. A. Pople, M. Ratner, T. L. Windus, *J. Chem. Phys.* **1998**, *109*, 1223–1229.
[47] A. R. Allouche, *J. Comput. Chem.* **2011**, *32*, 174–182.

Received: December 2, 2014

 © 0000 Wiley-VCH Verlag GmbH & Co. KGaA, Weinheim

EurJIC European Journal of Inorganic Chemistry

Iron Nitrosyl Chemistry

Keywords: Iron / Nitrogen oxides / Diimines / Electrochemistry / IR spectroscopy

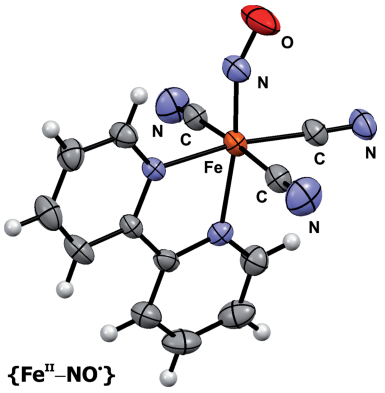

The previously reported complex [Ph_4P][Fe(bpy)$(CN)_3$(NO)] (bpy = 2,2′-bipyridine) was synthesised and a detailed structural (single-crystal XRD), (spectro)-electrochemical and spectroscopic insight is provided that adds perfectly to the previous electrochemical characterisation.

 © 0000 Wiley-VCH Verlag GmbH & Co. KGaA, Weinheim